TIEG1 deficiency confers enhanced myocardial protection in the infarcted heart by mediating the Pten/Akt signalling pathway

MINGQIU CEN[1], PENGFEI HU[2], ZHAOBIN CAI[1], TIANFU FANG[1], JIANCHENG ZHANG[3] and MING LU[2]

[1]Department of Cardiology, Xixi Hospital of Hangzhou, Hangzhou, Zhejiang 310023; Departments of [2]Cardiology and [3]Emergency Medicine, The Second Affiliated Hospital of Zhejiang Chinese Medical University, Hangzhou, Zhejiang 310005, P.R. China

Received March 1, 2016; Accepted January 19, 2017

DOI: 10.3892/ijmm.2017.2889

Abstract. The transforming growth factor (TGF)-β-inducible early gene-1 (TIEG1) plays a crucial role in modulating cell apoptosis and proliferation in a number of diseases, including pancreatic cancer, leukaemia and osteoporosis. However, the functional role of TIEG1 in the heart has not been fully defined. In this study, we first investigated the role of TIEG1 in ischaemic heart disease. For *in vitro* experiments, cardiomyocytes were isolated from both TIEG1 knockout (KO) and wile-type (WT) mice, and the apoptotic ratios were evaluated after a 48-h ischaemic insult. A cell proliferation assay was performed after 7 days of incubation under normoxic conditions. In addition, the angiogenic capacity of endothelial cells was determined by tube formation assay. For *in vivo* experiments, a model of myocardial infarction (MI) was established using both TIEG1 KO and WT mice. Echocardiography was performed at 3 and 28 days post-MI, whereas the haemodynamics test was performed 28 days post-MI. Histological analyses of apoptosis, proliferation, angiogenesis and infarct zone assessments were performed using terminal deoxynucleotidyltransferase-mediated dUTP nick-end labelling (TUNEL) staining, BrdU immunostaining, α-smooth muscle actin (α-SMA)/CD31 immunostaining and Masson's trichrome staining, respectively. Changes in the expression of related proteins caused by TIEG1 deficiency were confirmed using both reverse transcription-quantitative polymerase chain reaction (RT-qPCR) and western blot analysis. Our results demonstrated that the absence of TIEG1 prevented cardiomyocytes from undergoing apoptosis and promoted higher proliferation; it stimulated the proliferation of endothelial cells *in vitro* and *in vivo*. Improved cardiac function and less scar formation were observed in TIEG1 KO mice, and we also observed the altered expression of phosphatase and tensin homolog (Pten), Akt and Bcl-2/Bax, as well as vascular endothelial growth factor (VEGF). On the whole, our findings indicate that the absence of TIEG1 plays a cardioprotective role in ischaemic heart disease by promoting changes in Pten/Akt signalling.

Correspondence to: Dr Ming Lu, Department of Cardiology, The Second Affiliated Hospital of Zhejiang Chinese Medical University, 318 Chaowang Road, Hangzhou, Zhejiang 310005, P.R. China
E-mail: zbz1375@sina.com

Key words: transforming growth factor-β-inducible early gene-1, myocardial infarction, apoptosis

Introduction

Myocardial infarction (MI) is the leading cause of morbidity and mortality worldwide, and extended ischaemia leads to irreversible myocardial damage (1,2), which results in pathological ventricular remodelling (3). Therefore, strategies with which to reduce the myocardial injury have been the focus of studies on MI (4,5).

The transforming growth factor-β (TGF-β)-inducible early gene-1 (TIEG1), also known as Kruppel-like factor 10, was first discovered in foetal osteoblasts using a polymerase chain reaction (PCR) assay (6). TIEG1 expression is induced by TGF-β, bone morphogenetic proteins (BMPs) and other cytokines (7). It is located in multiple cell types and tissues, such as myocytes, tumour tissues and osteoblasts (8,9). The TIEG1 gene encodes a 72 kDa protein, which regulates cell growth and apoptosis (10,11). There has been significant progress regarding the role of TIEG1 in various diseases. In the field of cancer studies, Yao *et al* found that TIEG1 blocked the proliferation and induced the apoptosis of leukaemic cell lines, including HL-60, U937, Raji and K562 in both a time- and dose-dependent manner (12). Jiang *et al* proved that the transactivation of TIEG1 inhibited the growth of hepatocellular carcinoma cells in a dose-dependent manner (13). Moreover, Jin *et al* demonstrated that TIEG1 inhibited the invasion and metastasis of breast cancer by suppressing epidermal growth factor receptor (EGFR) transcription and the EGFR-related signalling pathway (14). However, the biological function of TIEG1 in the cardiovascular field remains unclear. In 2011, Miyake *et al* discovered that TIEG1 was a feedback regulator of myostatin in myoblasts (9), and Li *et al* illustrated that TIEG1 played a novel role as a blocker in angiotensin II (Ang II)-induced hypertrophy via the GATA binding protein 4 (GATA4) signalling pathway (15).

In this study, we investigated both the functional changes and underlying pathway variations caused by TIEG1 deficiency

in ischaemic heart disease, in both *in vitro* and *in vivo* experiments in an aim to fully determine the role of TIEG1 in heart disease.

Materials and methods

Experimental animals. All animal experiments were approved by the Animal Care and Use Committee of Zhejiang Chinese Medical University, Hangzhou, China and met the guidelines for the Care and Use of Laboratory Animals published by the National Institutes of Health. Wild-type (WT) C57BL/6 and 10 TIEG1 knockout (KO) mice (aged 6-8 weeks; C57BL/6 background) were purchased from Nanjing University, Nanjing, China for research purposes only. The mice were housed in cages in a controlled environment (12 h light/dark) with an ambient humidity of 50-80% and a temperature of 21±4˚C. Food and water were available *ad libitum*.

Isolation of neonatal ventricular cardiomyocytes (CMs). Neonatal ventricular CMs were prepared as described previously (16,17). Briefly, the hearts from 10 other 24-h-old TIEG1 KO and WT mice were removed and dissociated with 0.1% trypsin (Gibco, Grand Island, NY, USA). The dispersed cells were cultured with 10% fetal bovine serum (FBS)-supplemented high glucose Dulbecco's modified Eagle's medium (DMEM) (glucose concentration, 4 g/l) at 37˚C with 5% CO_2 for 90 min. Unadherent cells were harvested and seeded on the bottom of 24-well plates ($2.5x10^5$ cells/well) or 6-well plates ($1x10^6$ cells/well).

Isolation of endothelial cells. Murine endothelial cells were isolated from 10 WT and TIEG KO adult mice as previously described (18) with some modifications. The mice were sacrificed by an overdose of isoflurane, the lungs were separated and minced into small pieces, washed in Hank's buffer and digested with dispase for 1 h. The homogenate was passed through a filter and centrifuged at 300 x g for 5 min. The resulting cells were suspended and purified with anti-mouse VE-cadherin antibody-coated magnetic beads (BD Pharmingen, Heidelberg, Germany). The collected cells were cultured in DMEM (Invitrogen, Darmstadt, Germany) supplemented with 20% fetal calf serum, endothelial cell growth factor (Sigma-Aldrich, St. Louis, MO, USA) penicillin (50 U/ml) and streptomycin (50 μg/ml). The endothelial cells from the first two passages were >95% Dil-Ac-LDL positive for purification. The cells at passage 3-6 were then prepared for use in the *in vitro* experiments.

In vitro apoptosis assay. The neonatal CMs were seeded at $1x10^4$ cells/well in 24-well plates and apoptosis was induced under hypoxic conditions (0.1% O_2, 5% CO_2) in FBS-free medium for 48 h. The apoptotic cells were detected by terminal deoxynucleotidyltransferase-mediated dUTP nick-end labelling (TUNEL) staining (In Situ Cell Death kit, TMR red; Roche Applied Science, Indianapolis, IN, USA). Briefly, the cells were fixed in 4% paraformaldehyde, permeabilised in 0.2% Triton X-100, blocked with 5% BSA and incubated with primary antibodies [troponin I (TnI; ab47003); Abcam, Cambridge, MA, USA] overnight followed by the respective fluorescent conjugated secondary antibodies [goat anti-rabbit IgG H&L (DyLight 488; ab96883); and goat anti-rabbit IgG H&L (DyLight 550; ab96884); both from Abcam]. Following 3 washes with 0.1% Tween-20 phosphate-buffered saline (PBS), the CMs were incubated with the reaction mixture provided with the TUNEL kit following the manufacturer's instructions. Cell nucleuses were stained with 4',6-diamidino-2-phenylindole, dihydrochloride (DAPI) (Thermo Fisher Scientific, Waltham, MA, USA). Fluorescence images were acquired using a Leica fluorescence microscope (Leica, Wetzlar, Germany).

In vitro proliferation assay. Cell proliferation was determined by Ki67 immunostaining. Neonatal CMs were seeded at $1x10^4$ cells/well in 24-well plates and cultured under normoxic conditions (37˚C, 5% CO_2, 5% O_2) for 7 days. The proliferating cells were detected by double staining with Ki67 and TnI. Briefly, the cells were fixed in 4% paraformaldehyde, blocked with 5% BSA after 10 min of permeabilization, and incubated with primary antibodies [Ki67 (ab16667), TnI (ab30807) both from Abcam] overnight followed by the respective fluorescent conjugated secondary antibodies [donkey anti-rabbit IgG H&L (DyLight 488; ab96891); and donkey anti-goat IgG H&L (DyLight 550; ab96932); both from Abcam]. After 3 washes with PBST, the cell nuclei were stained with Hoechst 33258 pentahydrate 1 μg/ml (Invitrogen). Fluorescence images were then acquired using a Leica fluorescence microscope.

Tube formation assay. To investigate the angiogenic potential of endothelial cells *in vitro*, the cells were seeded at a concentration of $2x10^4$ cells onto each growth factor-reduced Matrigel (BD Pharmingen, San Diego, CA, USA)-coated well of a 96-well plate. Following 4-6 h of incubation, the capillary network structures of the endothelial cells were photographed using a phase-contrast microscope (Leica, Wetzlar, Germany), and the total number of inter-branches was evaluated using Image-Pro software.

Mouse model of MI. All animal research protocols met with the National Institutes of Health (NIH) Publication no. 85-23, (revised in 1996) and were approved by the Animal Care and Use Committee of Zhejiang Province Medical Institute. The WT and TIEG1 KO mice were subjected to MI as previously described (19,20). Briefly, the mice were anaesthetised intraperitoneally with pentobarbital sodium (60 mg/kg) and ventilated with a rodent ventilator via tracheal intubation. The hearts were exposed through a lateral thoracotomy, and the left anterior descending artery (LAD) was permanently ligated with a 7-0 silk suture. Paleness around and below the ligation point indicated a successful operation. The chest was closed, and the mice were placed back into cages following surgery.

Assessment of cardiac function by echocardiography and haemodynamics. Echocardiography was performed at 3 and 28 days post-MI, whereas haemodynamics evaluation was performed 28 days post-MI. Briefly, the mice were anaesthetised via the inhalation of isoflurane at a concentration of 2%, and a transthoracic parasternal M-mode echocardiogram was performed using a Vevo 2100 system. The left ventricular end-diastolic diameter (LVEDD and end-systolic diameter (LVESD) were obtained from at least 3 separate cardiac cycles. The

Table I. Name and sequence of primer sets for RT-qPCR.

Gene name	Primer sequence	Gene ID	Product size (bp)
Mus-TIEG1	F: CATCCGTCACACAGCTGATG	NM 013692.3	250
Mus-TIEG1	R:TGTCTCTGAGGAAGGCACAG		
Mus-Pten	F: GAAAGGGACGGACTGGTGTA	NM 008960.2	213
Mus-Pten	R:TCTTGTGAAACAGCAGTGCC		
Mus-Bcl-2	F: TTGTAATTCATCTGCCGCCG	NM 009741.5	179
Mus-Bcl-2	R:AATGAATCGGGAGTTGGGGT		
Mus-Bax	F: TCATGAAGACAGGGGCCTTT	NM 007527.3	197
Mus-Bax	R:GTCCACGTCAGCAATCATCC		
Mus-Casp-3	F: CAGCCAACCTCAGAGAGACA	NM 009810.3	190
Mus-Casp-3	R:ACAGGCCCATTTGTCCCATA		
Mus-GAPDH	F: CTGCGACTTCAACAGCAACT	NM 008084.3	330
Mus-GAPDH	R:GAGTTGGGATAGGGCCTCTC		

TIEG1, transforming growth factor-β-inducible early gene-1; Casp-3, caspase-3; GAPDH, glyceraldehyde-3-phosphate dehydrogenase; F, forward; R, reverse.

left ventricular end-systolic volume (LVESV) and left ventricular end-diastolic volume (LVEDV) were calculated as follows: 7.0 x $LVESD^3$/(2.4 + LVESD), and 7.0x $LVEDD^3$/(2.4 + LVEDD), respectively. The ejection fraction (EF, %) and fractional shortening (FS, %) were calculated as follows: [(LVEDV - LVESV)/LVEDV] x100, and [(LVEDD - LVESD)/LVEDD] x100, respectively.

Cardiac catheterization was performed with a catheter conducer (Millar Instrument, Houston, TX, USA) for haemodynamic assessment. A 1.4F pressure catheter, SPR-671, was inserted into the aorta and left ventricle through the right carotid artery. The transducer was connected to measure the left ventricular systolic pressure (LVSP), left ventricular end diastolic pressure (LVEDP), and left ventricular maximum ±dp/dt.

Histological analysis. The animals were sacrificed, and the excised hearts were immediately placed in a 10% KCl solution to induce cardiac arrest during the diastolic phase. The left and right atria of the heart were removed, leaving the left ventricle, and dehydrated in a 30% sucrose solution. The samples were embedded in Tissue-Tek OCT (Sakura Finetek, Torrance, CA, USA) compound and snap-frozen in liquid nitrogen. Frozen sections of the left ventricle were cut into a 7-μm-thick sections.

After preparing 3-day-post-MI samples, TUNEL assay was used to measure the ratio of CM apoptosis in the border zone according to manufacturer's instructions. The slices were fixed in 4% paraformaldehyde, permeabilised with 0.2% Triton X-100, blocked with 5% BSA and incubated with primary antibodies (TnI; Abcam) overnight followed by the respective fluorescent conjugated secondary antibodies. After 3 washes with 0.1% Tween-20 PBS, the sections were incubated in equilibration buffer accroding to the manufacturer's instructions. Nucleotide and TdT enzyme mixture were added to the samples at 37˚C for 1 h. Cell nuclei were stained with Hoechst 33258 pentahydrate 1 μg/ml (Invitrogen). Fluorescence images were obtained using a Leica fluorescence microscope. The ratio of TUNEL-positive CMs was analysed using the quantitative software Image-Pro Plus.

For BrdU incorporation assay, the 7 day-post-MI heart sections were fixed in 4% paraformaldehyde for 10 min, permeabilised in 0.2% Triton X-100, and blocked with 5% BSA in PBS for 1 h. The samples were incubated with primary antibody reacted with BrdU (ab1893, Abcam), which was injected into the heart on the day of the surgery and primary antibody to TnI (ab47003, Abcam) diluted 1:200 at 4˚C overnight, followed by incubation with the respective secondary fluorescent antibodies [donkey anti-sheep IgG H&L (DyLight 488; ab96939); and donkey anti-rabbit IgG H&L (DyLight 550; ab96892); both from Abcam]. Nuclei were stained with DAPI (Thermo Fisher Scientific), and imaging was observed using a fluorescence microscope (Leica, Wetzlar, Germany). The proportion of BrdU-positive CMs was analysed using the quantitative software Image-Pro Plus.

For α-smooth muscle actin (α-SMA)/CD31 immunostaining, the 7-day-post-MI heart tissue sections were fixed in 4% paraformaldehyde, permeabilised with 0.2% Triton X-100 and blocked with PBST containing 5% BSA. The samples were reacted with anti-α-SMA antibody (ab21027) and anti-CD31 antibody (ab7388) (both from Abcam) at 4˚C overnight. After several washes with PBST, the samples were reacted with fluorescence-conjugated secondary antibody for 1 h at room temperature. Cell nuclei were stained with Hoechst 33258 pentahydrate 1 μg/ml. The fluorescence photographs were obtained at 4-5 randomly selected high visual fields in the border zone of ischaemic myocardium/sample and calculated average number of microvessels/visual field with a Leica fluorescence microscope.

The scar size of the 28-day-post-MI samples was measured using Masson's trichrome staining. Briefly, the frozen tissue sections of heart tissues from different groups were fixed in

4% paraformaldehyde and stained with the Masson's trichrome kit (HT15, Sigma-Aldrich). The fibrosis and total left ventricular area of each image were measured using Image-Pro Plus software. The infarct area was calculated as the percentage (%) of the infarcted area divided by the entire left ventricle.

Reverse transcription-quantitative PCR (RT-qPCR). Total RNA was extracted from the CMs using TRIzol reagent (Invitrogen) according to the manufacturer's instructions. cDNA was synthesized from 2 μg of RNA using Moloney murine leukaemia virus (M-MLV) reverse transcriptase and an oligo$(dT)_{18}$ primer (Takara, Otsu, Japan). Quantitative PCR (qPCR) was performed using the SYBR-Green Reaction Mix (Takara) following the manufacturer's instructions. The PCR conditions were 95˚C for 10 min and 40 cycles of 95˚C for 30 sec, 60˚C for 30 sec and 40 cycles of 72˚C for 1 min. The PCR primers were designed using Primer3 Input online software and are listed in Table I. Glyceraldehyde-3-phosphate dehydrogenase (GAPDH) was used as a control, and the relative expression of the target genes were evaluated by a comparative CT method and normalised to the control.

Western blot analysis. After a 48-h incubation under hypoxic conditions and FBS-free stimulation, the CMs were rinsed with PBS, lysed in 2.5X sodium dodecyl sulfate (SDS) gel loading buffer [30 mM Tris-HCl (pH 6.8), 1% SDS, 0.05% bromophenol blue, 12.5% glycerol and 2.5% mercaptoethanol] and boiled for 30 min. We also rinsed the endothelial cells with PBS, lysed them in 2.5X SDS gel loading buffer [mM Tris-HCl (pH 6.8), 1% SDS, 0.05% bromophenol blue, 12.5% glycerol and 2.5% mercaptoethanol] followed by boiling for 30 min. Equal amounts of the cell lysates were loaded, and the proteins were separated on 8-12% SDS polyacrylamide gels and electrotransferred onto polyvinylidene fluoride (PVDF) membranes (Millipore, Boston, MA, USA). After the non-specific binding sites were blocked with 5% non-fat milk, the membranes were incubated with the primary antibodies, TIEG1 (1:500; A302-015A, Bethyl, Laboratories Inc., Montgomery, TX, USA), Pten (1:500; 9559), p-Akt (1:500; 13038), t-Akt (1:500; 14702), Bcl-2 (1:500; 3498), Bax (1:500; 2772), caspase-3 (1:500; 9664) (all from Cell Signaling Technology, Beverly, MA, USA), VEGF (1:500; Abcam) and actin (1:3,000; Kangchen, Shanghai, China), followed by horse radish peroxidase (HRP)-conjugated secondary antibody (sc-2357; Santa Cruz Biotechnology, Dallas, TX, USA) incubated at room temperature. After washing with PBST, the protein bands were visualised using the Gel Doc EZ Imaging System and analysed using Image Lab software (Bio-Rad, Hercules, CA, USA).

Statistical analysis. All the data are presented as the means ± standard deviation (SD). Statistical analyses for the measurement of significant differences between the TIEG1 KO and WT groups were performed using the Student's t-test. Probability values of $P<0.05$ were considered to indicate statistically significant differences.

Results

Suppression of TIEG1 results in decreased apoptosis in vitro. To examine the biological role of TIEG1 in CM apoptosis, CMs isolated from TIEG1 KO and WT mice underwent 48 h of exposure to hypoxic conditions. We evaluated TUNEL-positive cells and found that TIEG1 deficiency led to an approximately 15% decrease in the apoptosis of myocytes in the border areas compared to the WT group ($P<0.05$; Fig. 1A and D).

Deficiency of TIEG1 results in increased CM proliferation in vitro. To determine the functional role of TIEG1 in CM proliferation, Ki67 immunostaining was performed. We calculated the number of Ki67-positive cells and found that TIEG1 deficiency led to a 20% greater number of proliferative CMs than the WT mice ($P<0.05$; Fig. 1B and E).

Absence of TIEG1 results in the promotion of the proliferation of endothelial cells in vitro. To determine the functional role of TIEG1 in endothelial cell proliferation, tube formation was performed. We calculated the length of capillary structure in the TIEG1 KO and WT group, and found that the endothelial cells from the TIEG1 KO mice had a greater powerful ability of microvessel formation than those from the WT mice ($P<0.05$; Fig. 1C and F).

Deletion of TIEG1 ameliorates cardiac function and decreases infarct size in vivo. To determine whether TIEG1 plays a key role in cardiac function, we evaluated the myocardial contractile parameters at 3 and 28 days post-MI in mice. The echocardiographic results indicated that the absence of TIEG1 led to an improvement in heart function compared to the WT group at 28 days post-MI (Fig. 2A), including a better EF (TIEG1 KO, 41.496±2.131%; WT, 27.616±2.503%), and FS (TIEG1 KO, 23.522±0.870%; WT, 17.536±1.585%) ($P<0.05$; Fig. 2B and C). Furthermore, the LVEDD and LVESD were shorter in the TIEG1 KO mouse hearts than in the WT group at 28 days post-MI (LVEDD: TIEG1 KO, 3.841±0.122 mm; WT, 4.165±0.108 mm; LVESD: TIEG1 KO, 2.950±0.133 mm; WT, 3.420±0.112 mm) ($P<0.05$; Fig. 2D and E). Moreover, the haemodynamic results revealed a similar effect. Compared to the WT group, the TIEG1 KO mice had a significantly higher LVSP, a lower LVEDP and a higher ±dp/dt (TIEG1 KO: LVSP, 125±12 mmHg; LVEDP, 2.4±0.8 mmHg; dp/dt, 11500±1050; -dp/dt, -9700±790 mm; WT: LVSP, 95±7 mmHg; LVEDP, 5.9±1.1 mmHg; dp/dt, 7800±1100; -dp/dt, -5400±850) ($P<0.05$; Fig. 2F-I).

To evaluate the effect of TIEG1 on infarct size variation, Masson's trichrome staining was used. The quantitative assessment of myocardial fibrosis indicated that the TIEG1-deficient mice had reduced 10% scar area compared to the WT group ($P<0.05$; Fig. 4A and B).

Lack of TIEG1 reduces apoptosis and enhances proliferation in vivo. We validated the role of TIEG1 in apoptosis *in vivo* using TUNEL staining in 3-day samples. Our findings revealed that the defect of TIEG1 markedly decreased the number of apoptotic nuclei in the border zone compared to the WT group ($P<0.05$; Fig. 3A and B).

The proliferation ratio of myocytes in the border area of 7-day-samples was measured by immunostaining with BrdU antibody. We observed more double-positive staining of BrdU and TnI ($P<0.05$; Fig. 3C and D) in the CMs in the border zones from the TIEG1 KO mice than those from the WT mice.

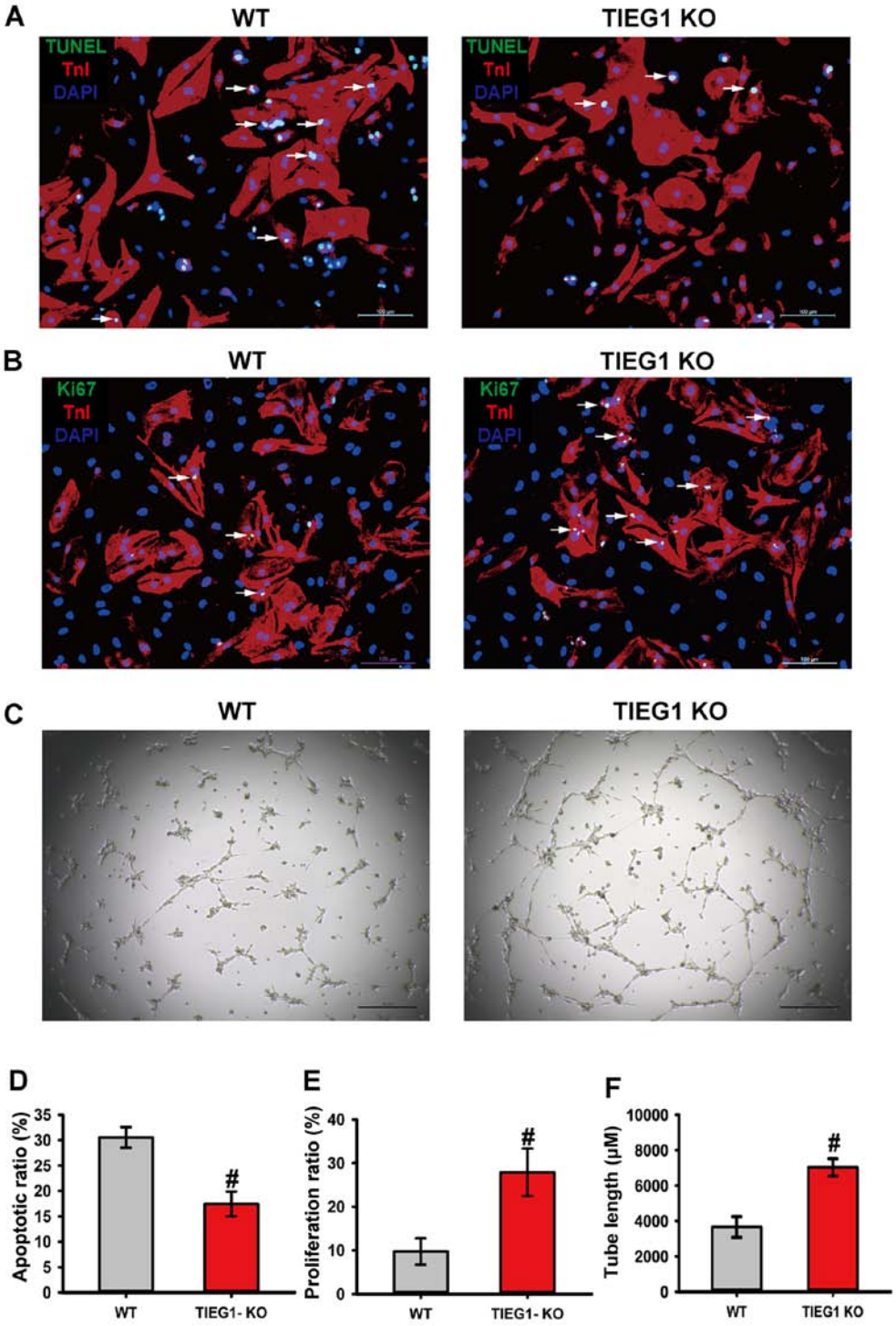

Figure 1. Deficiency of transforming growth factor-β-inducible early gene-1 (TIEG1) results in the decreased apoptosis and increased proliferation of cardiomyocytes (CMs) and endothelial cells *in vitro*. (A) Representive images of TUNEL-positive CMs (TUNEL-positive CMs are indicated by arrows). Scale bar denotes 100 μm. (B) Representive images of Ki67-positive CMs (Ki67-positive CMs are indicated by arrows). Scale bar denotes 100 μm. (C) Representive images of tube formation in endothelial cells. Scale bar denotes 100 μm. (D) Quantification of the apoptotic CMs (n=6/group). $^{\#}$P<0.01 vs. the WT group. (E) Quantification of the proliferative CMs (n=6 wells/group). $^{\#}$P<0.01 vs. the WT group. (F) Quantification of the length of tubes (n=6 wells/group). $^{\#}$P<0.01 vs. the WT group.

The absence of TIEG1 promotes angiogenesis in vivo. We validated the role of TIEG1 in angiogenesis *in vivo* using immunofluorescence staining in 28-day-samples. Our findings suggested that the defect of TIEG1 markedly increased microvessel formation in the border zone compared to the WT group (P<0.05; Fig. 3E-H).

Deficiency of TIEG1 influences the Pten/Akt and Bcl-2/Bax signalling pathways at both the mRNA and protein level in myocytes. In order to explore the underlying mechanisms responsible for the anti-apoptotic effects observed with the loss of TIEG1 in CMs, we analysed the relative expression levels of Pten/Akt and Bcl-2/Bax signalling pathway molecules

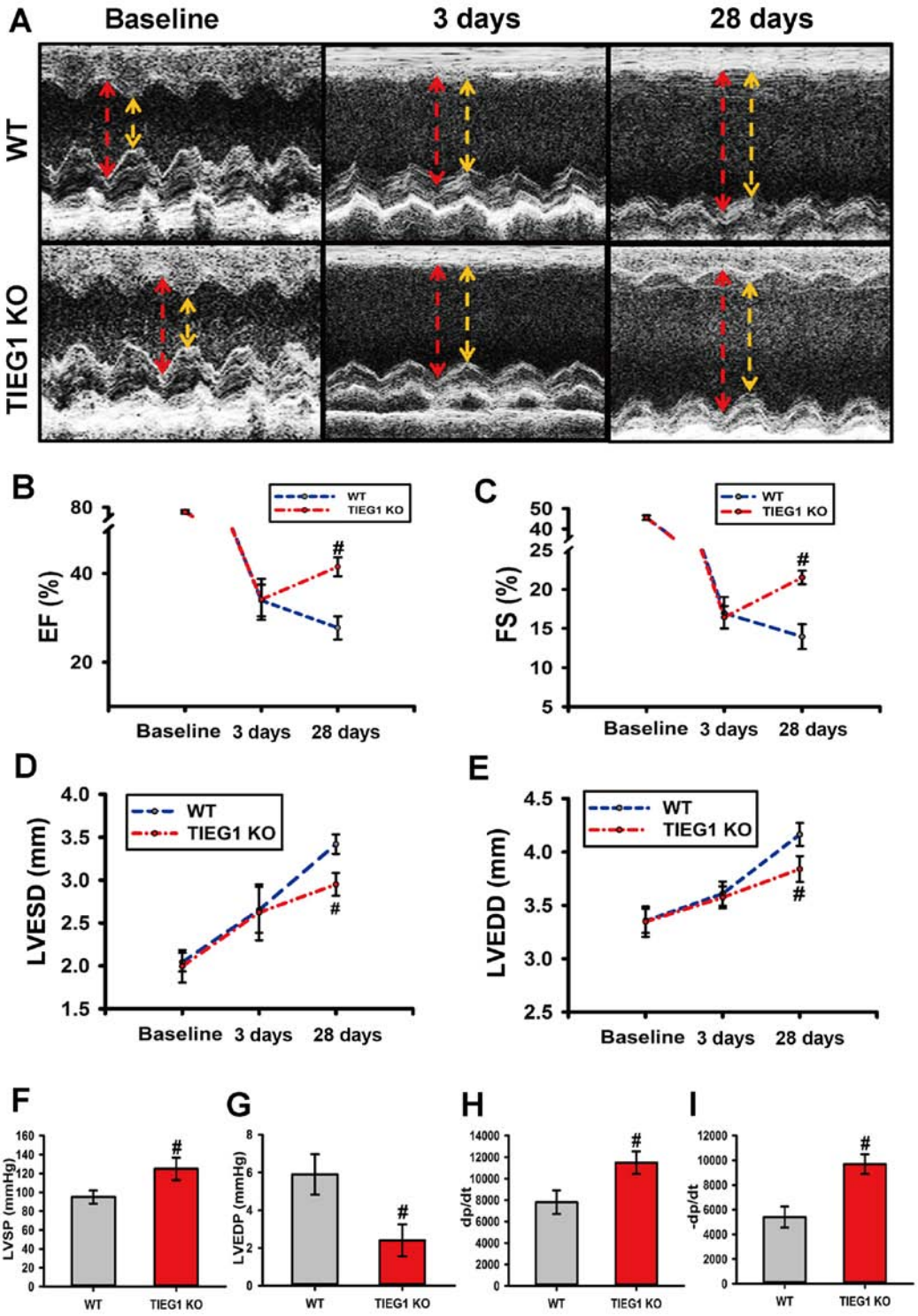

Figure 2. Deficiency of transforming growth factor-β-inducible early gene-1 (TIEG1) improves cardiac function. (A) Representative M-mode echocardiographic image. The yellow-dotted arrows represent LVESD and the red-dotted arrows represent LVEDD. (B-E) Quantitative analysis of echocardiography #P<0.01 vs. the WT group. EF, ejection fraction; FS, fractional shortening; LVESD, left ventricular end-systolic diameter; LVEDD, left ventricular end-diastolic diameter; LVSP, left ventricular systolic pressure. (F-I) Quantitative analysis of haemodynamics #P<0.01 vs. the WT group.

by RT-qPCR and western blot analysis. Our results revealed that a deficiency in TIEG1 led to the differential expression of the Pten/Akt and Bcl-2/Bax signalling pathway molecules at the mRNA and protein level. Specifically, the deficiency of TIEG1 decreased the expression of Pten, Bax and caspase-3, and increased the p-Akt/t-Akt ratio and the Bcl-2/Bax ratio (P<0.05; Fig. 4C-E).

Deficiency of TIEG1 influences the Pten/Akt and Bcl-2/Bax signalling pathways at both the mRNA and protein level in endothelial cells. We also examined the expression of related molecules in the Pten/Akt and Bcl-2/Bax signalling pathways in endothelial cells. Our results revealed the deficiency of TIEG1 also decreased Pten expression in endothelial cells, as in the CMs, and increased VEGF expression (P<0.05; Fig. 4F-H).

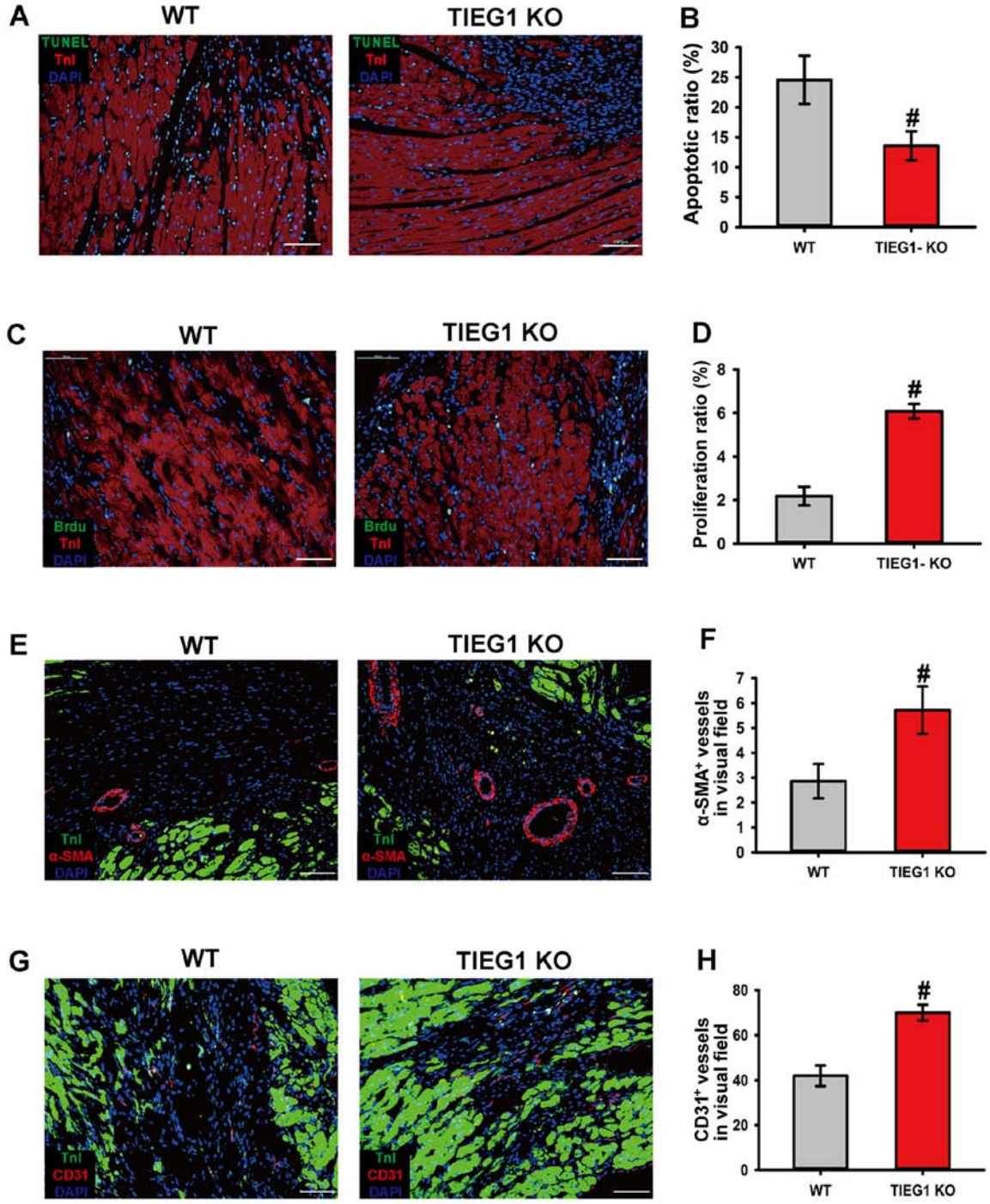

Figure 3. The lack of transforming growth factor-β-inducible early gene-1 (TIEG1) reduces apoptosis, enhances proliferation of cardiomyocytes (CMs) and stimulates neovascularization in the border zone. (A) Representative images of TUNEL-positive nuclei in CMs in the border zone. Scale bar denotes 100 μm. (B) Quantification of the apoptotic nuclei (n=6 samples/group). $^{\#}$P<0.01 vs. the WT group. (C) Representative images of BrdU-positive CMs in the border zone. Scale bar denotes 100 μm. (D) Quantification of the proliferative CMs (n=6 samples/group). $^{\#}$P<0.01 vs. the WT group. (E) Representative images of α-SMA-positive small arteries in the border zone. Scale bar denotes 100 μm. (F) Quantification of α-SMA-positive small arteries (n=6/group). $^{\#}$P<0.01 vs. the WT group. (G) Representative images of CD31-positive microvessels in the border zone. Scale bar denotes 100 μm. (H) Quantification of CD31-positive microvessels (n=6 samples/group). $^{\#}$P<0.01 vs. the WT group.

Discussion

Our study first assessed the role of TIEG1 in reducing myocardial damage and promoting microvessel generation in the infarcted heart. The major findings of our study are as follows: i) the lack of TIEG1 improves heart function and haemodynamics; ii) the absence of TIEG1 results in less myocardial apoptosis and greater myocyte proliferation, as shown by both *in vitro* and *in vivo* experiments; and iii) TIEG1 deficiency causes the variable expression of the Pten/Akt and Bcl-2/Bax signalling pathways; thus, these are the mechanisms through which TIEG1 deficiency has cardioprotective effects.

A number of studies have revealed the biological functions of TIEG1 in different cells (12,15,21). Of these properties, apoptosis induction and proliferation inhibition by TIEG1 have garnered attention from researchers. In the field of oncology,

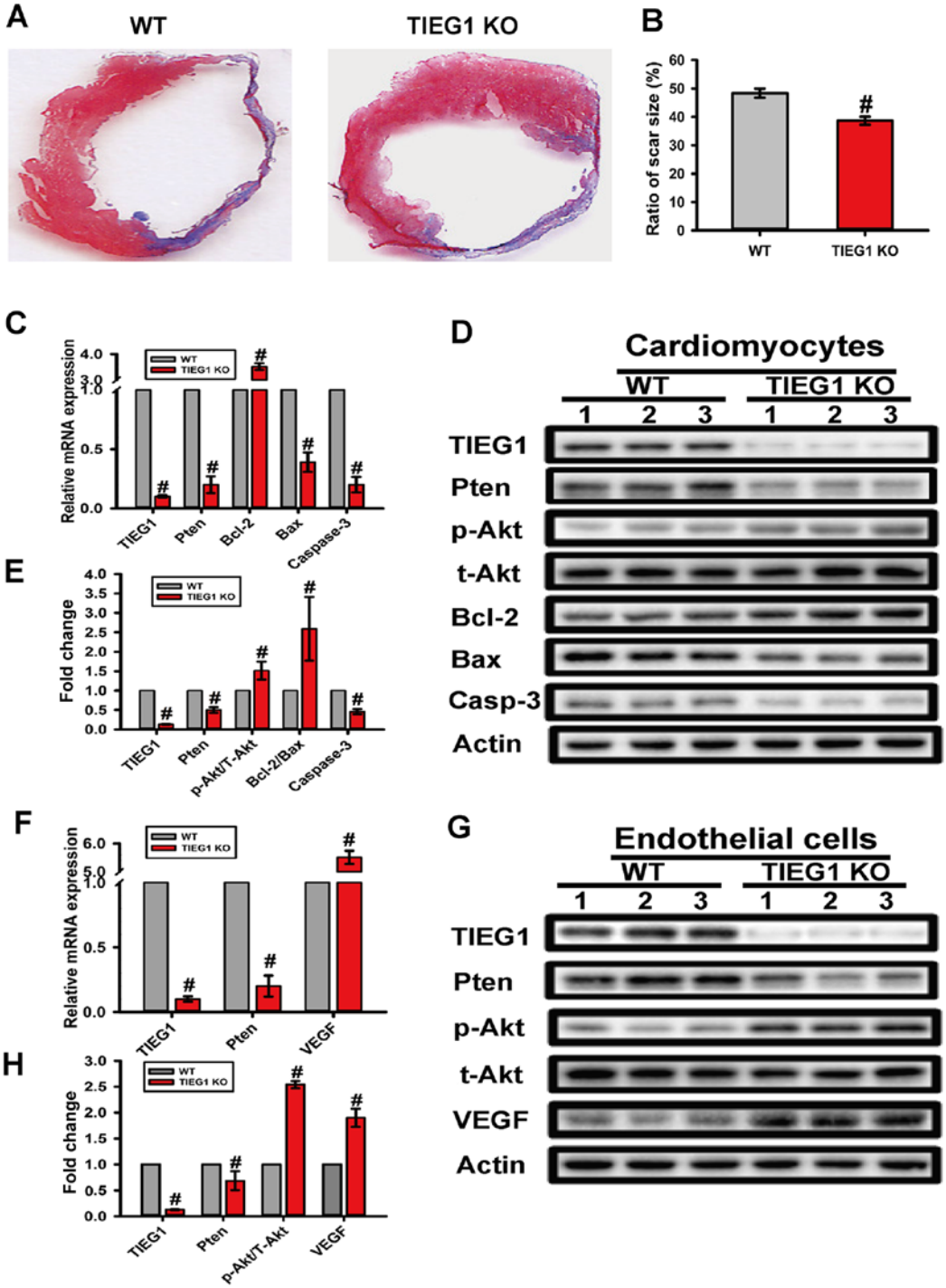

Figure 4. Deficiency of transforming growth factor-β-inducible early gene-1 (TIEG1) decreases infarct size, and alters the expression of molecules in the Pten/Akt and Bcl-2/Bax signalling pathways in myocytes and endothelial cells at the mRNA and protein level. (A) Representative Masson's trichrome staining of the heart to show the infarct zone 28 days post-myocardial infarction (MI). (B) Quantification of infarct zone in heart tissue. #P<0.01 vs. the WT group. (C) Quantitative analysis of mRNA expression of TIEG1, Pten, Akt, Bcl-2, Bax, caspase-3 in cardiomyocytes (CMs). #P<0.01 vs. the WT group. (D) Western blot analysis of the altered expression of Pten/Akt and Bcl-2/Bax signalling pathways in CMs. (E) Quantification of TIEG1, Pten, Akt, Bcl-2, Bax and caspase-3 expession in CMs, n=3. #P<0.01 vs. the WT group. (F) Quantitative analysis of mRNA expression of TIEG1, Pten, Akt, Bcl-2, Bax, caspase-3 in endothelial cells. #P<0.01 vs. the WT group. (G) Western blot analysis of the altered expression of Pten/Akt and Bcl-2/Bax signalling pathways in endothelial cells. (H) Quantification of TIEG1, Pten, Akt, Bcl-2, Bax and caspase-3 expession in endothelial cells, n=3. #P<0.01 vs. the WT group.

higher levels of TIEG1 protein have been shown to be expressed in epithelial cells compared to breast tumour cells, whereas it was absent in infiltrative tumour tissues, demonstrating its inhibitory role in cell growth (22). The results of haematological tumour analyses have also demonstrated the effects of TIEG1 (23,24). Jin *et al* found that TIEG1 is a key regulator that promotes the apoptosis of K562 leukaemic cells (25). Furthermore, TIEG1 has been shown to promote the apoptosis of different leukaemia cell lines, such as HL-60, U937, Raji and K562, in a dose- and time-dependent manner (12).

For cardiovascular diseases, TIEG1 was first reported to be involved in cardiac hypertrophy in 2007 (26), and this result was confirmed in a later clinic study (27). Currently, TIEG1 prevents CMs from Ang II-mediated hypertrophy, which provides a novel strategy for the treatment of cardiac hypertrophy (15). Although the effect of TIEG1 on hypertrophy has been studied, the functional role of TIEG1 in myocardial infarction remains unknown. In this study, we examined cell apoptosis and proliferation in the myocardium both *in vitro* and *in vivo*, in a TIEG1-deficient mouse model of MI compared to a WT mouse model of MI. Moreover, we characterised the heart function and haemodynamics of the TIEG1 KO mice and investigated the underlying pathway responsible for these phenotypic changes.

For our *in vitro* experiments, CMs from TIEG1 KO mice were significantly more resistant to apoptosis according to the results of TUNEL assay. By contrast, Ki67 immunostaining demonstrated that the lack of TIEG1 was also beneficial to myocyte proliferation. These results suggest the acceleration of apoptosis and the suppression of proliferation by TIEG1 in CMs, which have not been previously reported, at least to the best of our knowledge. Notably, our findings using the animal model of MI also revealed that the TIEG1 KO mice had better cardiac functional recovery than WT mice following coronary artery ligation surgery. The results of histological analysis confirmed greater myocardium preservation and a smaller scar area in the TIEG1 KO infarcted mouse heart than in the WT mouse hearts. Our results provide strong evidence for the apoptosis-promoting role of TIEG1 in CMs both *in vitro* and *in vivo*.

Apoptosis can be initiated by the mitochondria-mediated intrinsic pathway. This pathway is controlled by the Bcl-2 protein family, which is critical for regulating apoptosis and cell survival. Bcl-2 inhibits apoptosis by forming heterodimers with Bax, a pro-apoptotic protein, to stop its release (28). Bcl-2 and Bax are relevant to apoptosis in CMs, and they are apoptosis involved factors in myocytes under ischaemic conditions (29,30). A correlation between TIEG1 and Bcl/Bax in tumour cells has been confirmed (12); however, this remains unclear in cardiovascular cells.

The tumour suppressor gene, Pten, inactivates the signalling pathway by promoting protein phosphatase to reduce tumour cell growth and invasion (31,32). Similarly, Pten inhibition results in cardioprotective effects against ischaemia reperfusion injury of the myocardium by stimulating apoptotic survival signals (33). Furthermore, the inactivation of the Pten gene is regulated by transcriptional modification (34).

Pten and Bcl-2/Bax are associated with apoptosis, and they are critical apoptosis factors in CMs. In this study, we found an increased Bcl-2 expression, and decreased Bax and downregulated expression of Pten caused by TIEG1 deficiency at both the mRNA and protein level in CMs, which is key to protecting CMs against apoptosis. However, the details of this process require further investigation.

In conclusion, our data demonstrate that the deletion of TIEG1 results in a significant anti-apoptotic effect for myocardium salvage following ischaemic injury. The cardioprotective effects caused by TIEG1 defects are associated with variations in the expression of Pten, Akt and Bcl-2/Bax. These data suggest that TIEG1 may be a novel target for the effective therapy of MI.

References

1. Alpert JS, Thygesen K, Antman E and Bassand JP: Myocardial infarction redefined - a consensus document of the Joint European Society of Cardiology/American College of Cardiology Committee for the redefinition of myocardial infarction. J Am Coll Cardiol 36: 959-969, 2000.
2. Kitsis RN, Peng CF and Cuervo AM: Eat your heart out. Nat Med 13: 539-541, 2007.
3. White HD, Norris RM, Brown MA, Brandt PW, Whitlock RM and Wild CJ: Left ventricular end-systolic volume as the major determinant of survival after recovery from myocardial infarction. Circulation 76: 44-51, 1987.
4. Kanelidis A, Premer C, Lopez JG, Balkan W and Hare JM: Route of delivery modulates the efficacy of mesenchymal stem cell therapy for myocardial infarction: A meta-analysis of preclinical studies and clinical trials. Circ Res Dec 28: pii: CIRCRESAHA.116.309819, 2016.
5. Shiba Y, Gomibuchi T, Seto T, Wada Y, Ichimura H, Tanaka Y, Ogasawara T, Okada K, Shiba N, Sakamoto K, *et al*: Allogeneic transplantation of iPS cell-derived cardiomyocytes regenerates primate hearts. Nature 538: 388-391, 2016.
6. Subramaniam M, Harris SA, Oursler MJ, Rasmussen K, Riggs BL and Spelsberg TCL Identification of a novel TGF-beta-regulated gene encoding a putative zinc finger protein in human osteoblasts. Nucleic Acids Res 23: 4907-4912, 1995.
7. Haldar SM, Ibrahim OA and Jain MK: Kruppel-like factors (KLFs) in muscle biology. J Mol Cell Cardiol 43: 1-10, 2007.
8. Spittau B and Krieglstein K: Klf10 and Klf11 as mediators of TGF-beta superfamily signaling. Cell Tissue Res 347: 65-72, 2012.
9. Miyake M, Hayashi S, Iwasaki S, Uchida T, Watanabe K, Ohwada S, Aso H and Yamaguchi T: TIEG1 negatively controls the myoblast pool indispensable for fusion during myogenic differentiation of C2C12 cells. J Cell Physiol 226: 1128-1136, 2011.
10. Reinholz MM, An MW, Johnsen SA, Subramaniam M, Suman VJ, Ingle JN, Roche PC and Spelsberg TC: Differential gene expression of TGF beta inducible early gene (TIEG), Smad7, Smad2 and Bard1 in normal and malignant breast tissue. Breast Cancer Res Treat 86: 75-88, 2004.
11. Lee JJ, Park K, Shin MH, Yang WJ, Song MJ, Park JH, Yong TS, Kim EK and Kim HP: Accessible chromatin structure permits factors Sp1 and Sp3 to regulate human TGFBI gene expression. Biochem Biophys Res Commun 409: 222-228, 2011.
12. Yao K, Xing HC, Wu B, Li Y, Liao AJ, Yang W and Liu ZG: Effect of TIEG1 on apoptosis and expression of Bcl-2/Bax and Pten in leukemic cell lines. Genet Mol Res 14: 1968-1974, 2015.
13. Jiang L, Lai YK, Zhang JF, Chan CY, Lu G, Lin MC, He ML, Li JC and Kung HF: Transactivation of the TIEG1 confers growth inhibition of transforming growth factor-β-susceptible hepatocellular carcinoma cells. World J Gastroenterol 18: 2035-2042, 2012.
14. Jin W, Chen BB, Li JY, Zhu H, Huang M, Gu SM, Wang QQ, Chen JY, Yu S, Wu J and Shao ZM: TIEG1 inhibits breast cancer invasion and metastasis by inhibition of epidermal growth factor receptor (EGFR) transcription and the EGFR signaling pathway. Mol Cell Biol 32: 50-63, 2012.
15. Li Q, Shen P, Zeng S and Liu P: TIEG1 inhibits angiotensin II-induced cardiomyocyte hypertrophy by inhibiting transcription factor GATA4. J Cardiovasc Pharmacol 66: 196-203, 2015.
16. Ehler E, Moore-Morris T and Lange S: Isolation and culture of neonatal mouse cardiomyocytes. J Vis Exp: Sep 6(79): 2013. doi: 10.3791/50154.
17. Louch WE, Sheehan KA and Wolska BM: Methods in cardiomyocyte isolation, culture, and gene transfer. J Mol Cell Cardiol 51: 288-298, 2011.
18. Marelli-Berg FM, Peek E, Lidington EA, Stauss HJ and Lechler RI: Isolation of endothelial cells from murine tissue. J Immunol Methods 244: 205-215, 2000.
19. Xiao J, Moon M, Yan L, Nian M, Zhang Y, Liu C, Lu J, Guan H, Chen M, Jiang D, *et al*: Cellular FLICE-inhibitory protein protects against cardiac remodelling after myocardial infarction. Basic Res Cardiol 107: 239, 2012.
20. Sun Y, Yi W, Yuan Y, Lau WB, Yi D, Wang X, Wang Y, Su H, Wang X, Gao E, *et al*: C1q/tumor necrosis factor-related protein-9, a novel adipocyte-derived cytokine, attenuates adverse remodeling in the ischemic mouse heart via protein kinase A activation. Circulation 128 (Suppl 1): S113-S120, 2013.
21. Subramaniam M, Pitel KS, Withers SG, Drissi H and Hawse JR: TIEG1 enhances Osterix expression and mediates its induction by TGFbeta and BMP2 in osteoblasts. Biochem Biophys Res Commun 470: 528-533, 2016.

22. Subramaniam M, Hefferan TE, Tau K, Peus D, Pittelkow M, Jalal S, Riggs BL, Roche P and Spelsberg TC: Tissue, cell type, and breast cancer stage-specific expression of a TGF-beta inducible early transcription factor gene. J Cell Biochem 68: 226-236, 1998.
23. Noti JD, Johnson AK and Dillon JD: The leukocyte integrin gene CD11d is repressed by gut-enriched Kruppel-like factor 4 in myeloid cells. J Biol Chem 280: 3449-3457, 2005.
24. Noti JD, Johnson AK and Dillon JD: The zinc finger transcription factor transforming growth factor beta-inducible early gene-1 confers myeloid-specific activation of the leukocyte integrin CD11d promoter. J Biol Chem 279: 26948-26958, 2004.
25. Jin W, Di G, Li J, Chen Y, Li W, Wu J, Cheng T, Yao M and Shao Z: TIEG1 induces apoptosis through mitochondrial apoptotic pathway and promotes apoptosis induced by homoharringtonine and velcade. FEBS Lett 581: 3826-3832, 2007.
26. Rajamannan NM, Subramaniam M, Abraham TP, Vasile VC, Ackerman MJ, Monroe DG, Chew TL and Spelsberg TC: TGFbeta inducible early gene-1 (TIEG1) and cardiac hypertrophy: Discovery and characterization of a novel signaling pathway. J Cell Biochem 100: 315-325, 2007.
27. Bos JM, Subramaniam M, Hawse JR, Christiaans I, Rajamannan NM, Maleszewski JJ, Edwards WD, Wilde AA, Spelsberg TC and Ackerman MJ: TGFβ-inducible early gene-1 (TIEG1) mutations in hypertrophic cardiomyopathy. J Cell Biochem 113: 1896-1903, 2012.
28. Cory S and Adams JM: The Bcl2 family: Regulators of the cellular life-or-death switch. Nat Rev Cancer 2: 647-656, 2002.
29. Cook SA, Sugden PH and Clerk A: Regulation of bcl-2 family proteins during development and in response to oxidative stress in cardiac myocytes: Association with changes in mitochondrial membrane potential. Circ Res 85: 940-949, 1999.
30. Misao J, Hayakawa Y, Ohno M, Kato S, Fujiwara T and Fujiwara H: Expression of bcl-2 protein, an inhibitor of apoptosis, and Bax, an accelerator of apoptosis, in ventricular myocytes of human hearts with myocardial infarction. Circulation 94: 1506-1512, 1996.
31. Myers MP, Stolarov JP, Eng C, Li J, Wang SI, Wigler MH, Parsons R and Tonks NK: P-TEN, the tumor suppressor from human chromosome 10q23, is a dual-specificity phosphatase. Proc Natl Acad Sci USA 94: 9052-9057, 1997.
32. Tamura M, Gu J, Matsumoto K, Aota S, Parsons R and Yamada KM: Inhibition of cell migration, spreading, and focal adhesions by tumor suppressor PTEN. Science 280: 1614-1617, 1998.
33. Ruan H, Li J, Ren S, Gao J, Li G, Kim R, Wu H and Wang Y: Inducible and cardiac specific PTEN inactivation protects ischemia/reperfusion injury. J Mol Cell Cardiol 46: 193-200, 2009.
34. Liu Y, Nie H, Zhang K, Ma D, Yang G, Zheng Z, Liu K, Yu B, Zhai C and Yang S: A feedback regulatory loop between HIF-1α and miR-21 in response to hypoxia in cardiomyocytes. FEBS Lett 588: 3137-3146, 2014.